Imperial College London
Faculty of Natural Sciences
Department of Theoretical Physics

MSc Quantum Fields and Fundamental Forces

Quantum Field Theory on Causal Sets Beyond 2D

Author:
Danny W. Prosser

Supervisors:
Dr. Yasaman Kouchekzadeh Yazdi

Student ID: 01986827
Date: 23/09/2021

A thesis submitted in partial fulfilment of the requirements for the degree of Master of Science of Imperial College London, 2020-2021.

Abstract

This thesis extends the work of Johnston [19] and Yazdi [21] by considering scalar quantum field theories defined on a 3-dimensional causal diamond. The Pauli-Jordan operator is defined for both discrete and continuous space-times and it's eigen-decomposition is calculated using causal set methods. The results from the discrete theory are then discussed in relation to possible solutions for the corresponding continuous case.

Acknowledgements

Thank you to my supervisor Dr Yasaman Yazdi for introducing me to causal sets and for all your patience, understanding and guidance over the last few months.

I would also like to thank Aaron Routh and Rushit Mehmeti for sharing the last four years with me. I am particularly grateful to have studied with you both at Imperial. Your continuing support has benefited me immeasurably and I could not ask for better friends.

Finally I would like to thank my parents for their unwavering belief in me.

Contents

List of Figures

Introduction

The main goal of 21st century Theoretical Physics, in one form or another, has been to unite the ideas of General Relativity (GR) and Quantum Field Theory (QFT) - the two most successful scientific theories to date. It is believed that at some small distance (high frequency) scale (at minimum the Plank scale $\sim 10^{-23}$cm), the gravitational fields of Einstein must produce quantum fluctuations if they are to properly describe the manifestation and propagation of matter which we observe. Over the course of the last sixty years many theories have been developed with the aim of unifying these two pillars of modern Physics; most notably, String Theory and Loop Quantum Gravity etc see [1–3] . Causal Set Theory (CST) is another such theory that has the advantage of being based on a simple set of axioms, derived from the causal structure of space-time, and reconstructs from these the laws of nature we observe in the universe. Causal set theory, in effect, is the idea that space-time itself is fundamentally discrete. In so far that a space-time manifold is the large scale approximation of a countable number of individual space-time elements - in which each element is related to another by its causal relationship. For more on the foundations of causal set theory see [4–9].

In fact, the idea that space and time could be discrete concepts is not a new one, and has been a problem pondered by many mathematicians and physicists from Riemann to Einstein. But it is how these elements relate to one another - in order to produce the complex structures we observe in the universe - which is of greatest interest. Thanks to the work done by Hawking and Ellis [10] it is known that in order to recover the conformal metric of any space-time one only needs information about the causal nature or distribution of light-cones within that space. Once one knows the conformal metric then all that is left is to define a suitable scale factor to retrieve the complete metric of the space. It is based on this knowledge that Rafael Sorkin coined the term "Order + Number = Geometry". Pairing the ideas of discreteness and causality into a picture of space-time as a set of elements endowed with a partial ordering (a poset), which implements the causal relations between elements, one arrives at causal set theory. The question remains, however, if nature does indeed exhibit the type of fundamental discreteness described above.

There are many open questions in modern physics which lay just outside our current knowledge, in which only a theory of Quantum Gravity will suffice to answer. Some of these problems we know very little about, but for others there is enough information available to us that we can begin to test possible candidate theories in these regimes. The study of Black holes is one of these areas, and as such Black holes have garnered much interest from both the theoretical and experimental community over recent decades. The exterior of a Black hole is in a sense the border of our current knowledge, and for this reason it is a rich environment to look for clues about a deeper theory of nature. With this in mind we turn our attention to Black Hole entropy, to see if a discrete theory of space-time is applicable within this framework.

It is known that the entropy of a black hole obeys an area law, whereby the area is defined to be the area of the event-horizon of the black hole [11–13]. However, if our current understanding is correct, the space-time in which the black hole manifests is the same either side of the event-horizon. In fact, an observer passing through an even horizon of a black hole would not be able to distinguish the difference between the exterior and interior - the difference being a purely causal one. That is, anything inside the black hole event-horizon may not effect the anything to the exterior of the horizon. Here we have two separate, causally distinguishable, regions of space-time. The border of which being the area of the event horizon - the same area which determines the entropy of the black hole. Since the event-horizon is not anything other than a border of causally separated space-times, one is led to the conclusion that the area must surely be a measure of the space-time itself. Then, if the only thing distinguishing the two regions of space-time is a space-time surface - that surface resulting in a finite area law for the entropy of a black hole - then it

is natural to assume that space-time itself must be made up of a (possibly infinite) collection of finite sub-volumes; the connections between these different patches of space-time being determined by the causal structure of the space. Indeed, this line of reasoning was one of the main drivers in the development of causal set theory. Work has since been done to describe black hole entropy from causal sets in which it is proposed that the entropy comes from the number of links crossing the horizon [14]. Research into 2-dimensional causal diamonds in $\mathbb{M}^2$ also recovers an area law for space-time entanglement entropy [15].

The potential for causets to be a possible candidate for nature when considering black hole entropy has been eluded to above, but applying the idea of a causal set to other theories also shows promise. The most immediate application is to the problem of the infinities one encounters when re-normalising quantum field theories. However, a discrete space-time inherently supplies a small distance, or UV cut-off for the theory, see [16]. Also, by applying the ideas of causets to other areas of research new solutions may be found for existing problems with experimentally verifiable predictions. Cosmology is one such area of research where causets may offer new insights. Indeed, using a causal set framework a heuristic description of the origin of the cosmological constant has been outlined by R.Sorkin [17], and further work within Cosmology is being undertaken with regard to the evolution of universes, see [18].
Developments have also been made by Sorkin and Johnston in setting up a method for realising quantum fields on a fixed causal set background [19, 20]. Within the framework outlined by Johnston further analysis has been carried out by Yazdi [21], where it has been shown that in 2-dimensions the causal set approach does indeed agree with the continuum - in the large density limit - when compared to analytic results know for the continuum case . These approaches have worked with scalar quantum field theories in flat Minkowski space. However, work is also being undertaken to define an action principle for scalar fields on causal sets approximating curved space-times, See [22].

The aim of the current work is to expand on the results in [21] to further our understanding of the relationship between continuum and discrete scalar quantum field theories in flat Minkowski space. We do this by studying causets in $2+1$ dimensional $\mathbb{M}^3$. We also hope to learn more about the structure of the continuum theory by using causal sets as a guide. In fact, it is often much easier to work with causal sets to find approximate or limiting results - which can prove difficult to find analytically in continuum theories. In this regard even if nature is not fundamentally a causal set, we can nevertheless use computational methods to provide insights for continuum QFT.
We start in Chapter 2 by introducing some of the key mathematical and conceptual structure of CST in more detail, before going on to review the relevant theorems and results from Johnston and Yazdi. We briefly talk about how one might arrive at a causal set which could represent a Lorentzian manifold and discuss current work within this field of research. In Chapter 3 we turn our attention to the 3-dimensional causal diamond and approach the problem from both the causal set and continuum view point. We set up a causal set and calculate the eigenvalues and eigenfunctions of quantum mechanical operators on this set, analogously to the work done by [21] in $\mathbb{M}^2$. We then use these results to try and predict the form of their continuum counterparts which are yet to be determined analytically. Finally, we conclude with some remarks about what we have found and discuss further avenues of research regarding causal sets in $2+1$ dimensions and beyond.

Causal Set Theory

2.1 Principles of Causal Set Theory

Often when one tries to construct a model of the universe (or part of it) a good starting point is to first try to define a metric describing the space. From the metric one can recover the causal properties of the space-time [1]. It is this manifold picture of space-time that Einstein derived his field equations on - placing causality is at the heart of general relativity. However, when quantising such a theory one runs into various complications which arise from this picture [17]. Therefore, starting with a metric is fraught with difficulty if the goal is to then quantise gravity. However, it is known thanks to Hawking and Malament [23, 24], that one can retrieve the conformal metric just from information of the light-cones - in other words from the causal relationship (or order) between space-time points alone. This way of thinking elevates the role of causality and allows one to define a new topology away from the usual manifold like topology in which GR was first conceived. Therefore, with knowledge of the conformal scale factor - in essence a number - one can fully recover the metric of a Lorentzian space-time. Causal set Theory postulates a space-time constructed from a number of discrete elements whose relation to one another is defined by their causal order. Mathematically, a causal set is a set, $\mathcal{C}$ of endowed with a partial ordering, $\preceq$ which obeys the following axioms:

1. Reflective: $x \prec x$.

2. Transitivity: If $x \prec y$ and $y \prec z$, then $x \prec z \quad \forall\, x, y, z \in \mathcal{C}$.

3. No loops: If $x \prec y$ and $y \prec x$ then $x = y \quad \forall\, x, y \in \mathcal{C}$.

4. Finiteness: For any pair of points $x, z \in \mathcal{C}$, the set $\{y | x \prec y \prec z\}$ of elements between x and y is of finite size.

Here we distinguish $x \prec y$ to be where x causally precedes y written as $x \preceq y$ but where $x \neq y$. Transitivity ensures the causal structure is preserved throughout the set. The condition of 'no loops' is needed to exclude independent, self contained (possibly infinite) causal loops, which are both mathematically and philosophically undesirable features of a physical theory. Finally, finiteness relates to the assumption made that space-time volumes are taken to be finite - motivation for which was given in the previous chapter. More precisely this is the statement that the cardinality of the Alexandrov set between two elements is finite, or that $|| [v_1, v_2] || < \infty$, where $v_1, v_2 \in \mathcal{C}$. Given the conditions above which a causet must obey, one is immediately led to think about the dynamics of a causal set, and how one might retrieve a causal set which resembles a Lorentzian manifold. Key to this discussion is the conjecture that if a causal set resembles a Lorentzian manifold (M, g) then at large scales this mapping is unique, such that all other causal sets which also resemble (M, g) are equivalent. This is called the 'Hauptvermutung' conjecture. See also [25] for more a detailed discussion on how continuum topologies are recovered from causal sets.

[1] by which it is meant that one can find the light-cones at each point on the manifold

There are a number of different ways one might imagine causal set Kinematics and Dynamics. One such model for the emergence of these structures from causal sets is via a 'sequential growth model' (SGM) whereby new elements of a causal set are born from previous elements, and the set evolves to form a Lorentzian manifold-like structure [26, 27]. So far the work on SGMs is purely classical. However, the ideas discussed give one a picture of the type of processes required to form physically meaningful causal sets. Another approach led by Steven Wolfram and his team to describe the world from an initial finite number of elements endowed with simple update procedures has shown to be akin to some of the ideas of CST. These models are similar to SGMs but could possibly describe the quantum mechanical dynamics of causet-like objects, see [28] for a more in-depth discussion [2]. More work is required within the area of causet kinematics and for this project we will circumvent this by taking a different approach in setting up our causal set in 3D Minkowski space-time.
The approach adopted in this thesis is that of a 'sprinkling' of causal elements onto a 3D Minkowski manifold. A sprinkling is a process whereby elements of a given Lorentzian Manifold are selected randomly via a Poisson process of density ρ. These points are then taken to be the elements of the causet. By a Poisson process (or distribution) we mean that the probability of finding N points in a region of volume V is given by;

$$P(N) = \frac{(\rho V)^N}{N!} e^{-\rho V}. \tag{2.1}$$

The advantage of using a Poisson process is that the generated causet is manifestly Lorentz invariant [29]. Following a boost or rotation the points in the system are still randomly distributed, and therefore the system has no unique frame dependence. This is in opposition to the case of say Lattice field theory, where the lattice points are warped by the boots and a clear frame dependence exists. By utilising a Poisson process to generate the causet elements one also by-passes the subtleties of causal kinematics mentioned above.

2.2 Scalar Quantum Field Theory on a Causal Set

In the previous section we discussed how one could retrieve a causet of a Lorentzian Manifold via a sprinkling. What remains is how one proceeds to describe quantum mechanics, and more specifically QFT, in relation to the causet under study. In this regard we follow the methods developed by Johnston and Sorkin [19, 20]. We will work with a Gaussian QFT - one in which a wick rotation is well defined - in a globally hyperbolic space. If these two conditions are met then we may use the methods developed by Johnston and Sorkin to develop a QFT on our sprinkled causet. For future reference we will refer to this method as the Sorkin-Johnston method or SJ-QFT for short.

Next we introduce a number of key definitions which we will make extensive use of in the following sections. Namely, we introduce the causal and link Matrices - both of which are adjacency matrices. For a set $\mathcal{C}$ of finite length n endowed with a partial ordering $\prec$, we may represent the causet by an $n \times n$ matrix of two classes, either by;

The causal matrix,

$$C_{xy} := \begin{cases} 1 & \text{if} \quad v_x \prec v_y \\ 0 & \text{otherwise} \end{cases} \tag{2.2}$$

Or link matrix,

$$L_{xy} := \begin{cases} 1 & \text{if} \quad v_x \prec * v_y \\ 0 & \text{otherwise.} \end{cases} \tag{2.3}$$

Where $x, y = 1, 2, \ldots n$ and $v_1, v_2, \ldots v_n$ label the elements of $\mathcal{C}$. The symbol $\prec *$ denotes the nearest neighbour, such that if $x \prec y$ where $x, y \in \mathcal{C}$ and there exist no $w \in \mathcal{C}$ for which $x \prec w \prec y$ then x, y are called nearest neighbours and we write this $x \prec * y$. Before developing a quantum field theory on a causal set let us first review the basic approach when defining a quantum field theory in the continuum, and discuss what might happen if we try to apply these methods directly to causal sets.

[2] This research is still on-going but it is included nevertheless as interest for the reader.

2.2.1 Canonical Quantum Field Theory

A common approach, and often the simplest, is to set up a canonical quantum field theory. This is done by first solving the field equations, which for our case is just the Klein-Gordan equation for a scalar field

$$\left(\Box + m^2\right)\phi(\bar{x}) = 0, \tag{2.4}$$

where $\bar{x} = (t, x_1, x_2, x_3)$, and $\Box = \partial_\mu \partial^\mu = \eta^{\mu\nu}\partial_\mu\partial_\nu$. With signature $(-+++\dots)$ used throughout. From here one would seek to impose commutation relations on the field operator $\phi(\bar{x})$ and its momentum conjugate $\pi(\bar{x})$ such that for d-dimensional space-times ,

$$[\phi(\bar{x_1}), \pi(\bar{x_2})] = i\hbar\delta^d(x_1 - x_2) \tag{2.5}$$

$$[\phi(\bar{x_1}), \phi(\bar{x_2})] = 0, \qquad [\pi(\bar{x_1}), \pi(\bar{x_2})] = 0 \tag{2.6}$$

where $\delta(x_1 - x_2)$ is the Dirac-delta function as defined in [30]. Solutions for the fields ϕ which obey these conditions are usually expanded out in a basis of plane waves

$$\phi(\bar{x}) = \int \frac{dp^4}{(2\pi)^4}\left(\hat{a}(\bar{p})e^{-ix_\mu p^\mu} + \hat{a}^\dagger(\bar{p})e^{ix_\mu p^\mu}\right). \tag{2.7}$$

Imposing conditions (2.5) and (2.6) on (2.7) we get relations for $\hat{a}(\bar{p})$ and $\hat{a}^\dagger(\bar{p})$, in terms of $\phi(\bar{x})$ and $\pi(\bar{x})$, which allow us to identify them as so-called raising and lowering operators for positive and negative frequency states of the field respectively. All that remains is to define a suitable vacuum for the system $|0\rangle$ and then states of momentum p may be constructed by acting on the vacuum with $\hat{a}(\bar{p})^\dagger$ such that

$$|\bar{p}\rangle = \hat{a}(\bar{p})^\dagger|0\rangle \tag{2.8}$$

and,

$$|\bar{p}_1, \bar{p}_2, \dots \bar{p}_n\rangle = \hat{a}(\bar{p}_1)^\dagger\hat{a}(\bar{p}_2)^\dagger \dots \hat{a}(\bar{p}_n)^\dagger|0\rangle. \tag{2.9}$$

Operators defined in terms of $\phi(\bar{x})$ and $\pi(\bar{x})$ may then be calculated at any time via a time-evolution defined by the Hamiltonian of the system H, such that

$$\mathcal{O}(t, x) = e^{itH}\mathcal{O}(x)e^{-itH}. \tag{2.10}$$

For a full review of this procedure see [31]. It is the aim of causal set theory at this stage to agree with the continuum case, in the infinite density limit, if it to be a successful candidate theory of nature. Therefore, one would like to be able to compare results from both the discrete and continuous theories. However, due to the fundamental discretisation of the temporal structure of space-time the Hamiltonian is ill-defined - along with the phase-space mechanics upon which the theory rests. Therefore, one really wishes to define a QFT via a sum over histories or path integral method first devised by Dirac and then later formulated by Feynman [30, 32]. Progress has been made in defining a sum over histories formalism for scalar fields on causal sets, see [33], but a full description is still needed. With this in mind we wish to recast the theory into a framework of QFT that is defined through intrinsic space-time quantities and independent of the Hamiltonian. Such an approach has been developed by Johnston and Sorkin [19, 20]. Wherein the Greens function of the theory takes centre stage and is defined through a space-time volume [3]. The theory has also been shown by Dowker et al. [34] to be well defined by the proper time τ between space-time event, for which a discrete analogue exits in continuation of the stop-hop method introduced by Johnston.

2.2.2 Sorkin-Johnston QFT

We now introduce the construction developed by Johnston and Sorkin which utilises the Peierls bracket to determine the space-time propagator of a free massless scalar field in 1+2 dimensions in a manifestly covariant manner, without introduction of canonical variables [35]. We start by defining the retarded Greens function G_R^d in d-dimensions by requirement that it satisfy

[3] In the case of a causal set the sapce-time volume is defined as the number of causal elements within a region.

$$\left(\Box - m^2\right) G_R^d(x, x') = -\delta^{(d)}(x - x'). \tag{2.11}$$

If one also defines the Pauli-Jordan function to be

$$\triangle(x, x') := G_R(x, x') - G_A(x, x'), \tag{2.12}$$

where G_A is the advanced Greens function, which for a Gaussian theory is simply equal to the transpose of the retarded Greens function, such that $G_A(x, x') = G_R^T(x, x') = G_R(x', x)$. Then the commutator obeys

$$[\phi(x), \phi(x')] = i\triangle(x, x'). \tag{2.13}$$

Now $i\triangle$ is anti-symmetric and hermitian and admits positive and negative eigenvalues $\pm\lambda_i$. Working with a Gaussian quantum field theory it is sufficient to find a two-point function or Wightman function, from which all n-point correlation functions may be derived by Wick's theorem. If one takes only the positive part of $i\triangle$ it has been shown in [20] that one retrieves the Wightman function,

$$W := \mathrm{Pos}(i\triangle). \tag{2.14}$$

Since the eigenvalues of $i\triangle$ are comprised of positive and negative pairs $\pm\lambda_i$ the Wightman function may be expanded out as a sum of positive eigenvalues λ_i, along with a product of eigenfunctions u_i, such that

$$W = \sum_i \lambda_i u_i u_i^\dagger. \tag{2.15}$$

Now all that is left is to define the Feynman propagator in terms of the expressions we have defined above. From [36] we can find,

$$G_F = G_R - iW. \tag{2.16}$$

2.2.3 3D Continuous Theory

We start by looking at the SJ method applied to a 3-dimensional continuous theory. Unlike the 2-dimensional case previously studied - where an analytic solution of the continuum Pauli-Jordan function was found - no such analytic result has yet been found for 3-dimensions. Nevertheless, the form of the retarded greens function is known from [36] to be,

$$G_R^{(3)}(x, x') = \theta(\triangle t)\theta(\tau^2)\frac{1}{2\pi\tau}, \tag{2.17}$$

where τ is the proper time defined in the usual way such that $\tau^2 = \triangle t^2 - \triangle\vec{x}^2$. From (2.17) it would be desirable to calculate the Pauli-Jordan function via (2.12). Once we have found an expression for $\triangle$ within a space-time region V we can start looking for the eigenvalues and functions of $i\triangle$. One can achieve this by investigating the Hilbert space of square integrable functions $L^2(V)$ associated to V. We define the integral operator on functions within this space to be

$$(i\triangle\psi)(x) = \int_V dy\, i\triangle(x, y)\psi(y). \tag{2.18}$$

Thanks to (2.18) one may look for eigenfunctions of $i\triangle$ - as was demonstrated for $1+0$ and $1+1$ dimensions in [19]. Firstly, we would like to simplify (2.17) and the choice is now made to go to radial light-cone coordinates which are defined as follows,

$$t = \frac{1}{\sqrt{2}}(u + v), \tag{2.19}$$

$$x = \frac{1}{\sqrt{2}}(u - v)\cos\theta, \tag{2.20}$$

$$y = \frac{1}{\sqrt{2}}(u - v)\sin\theta. \tag{2.21}$$

The Jacobian for this transformation is calculated to be,

$$J = \begin{vmatrix} \frac{1}{\sqrt{2}} & \frac{1}{\sqrt{2}} & 0 \\ \frac{1}{\sqrt{2}}\cos\theta & -\frac{1}{\sqrt{2}}\cos\theta & -\frac{1}{\sqrt{2}}(u-v)\sin\theta \\ \frac{1}{\sqrt{2}}\sin\theta & -\frac{1}{\sqrt{2}}\sin\theta & \frac{1}{\sqrt{2}}(u-v)\cos\theta \end{vmatrix}, \\ = \frac{1}{\sqrt{2}}|u-v|. \tag{2.22}$$

Such that,

$$\iiint_V dtdxdy = \iiint_V \frac{1}{\sqrt{2}}|u-v|dvdud\theta, \\ = \int_0^{2\pi}\int_0^{\frac{h}{\sqrt{2}}}\int_0^{u}\frac{1}{\sqrt{2}}|u-v|dvdud\theta. \tag{2.23}$$

A visual representation of this change of variables is given in figure 2.1 where the boundaries of the causal diamond are shown to correspond to $u = h/2$ and $v = -h/2$ from equations (2.19), (2.20) and (2.21) along with a sprinkled causet of size $N = 2000$ and $h = 1$.

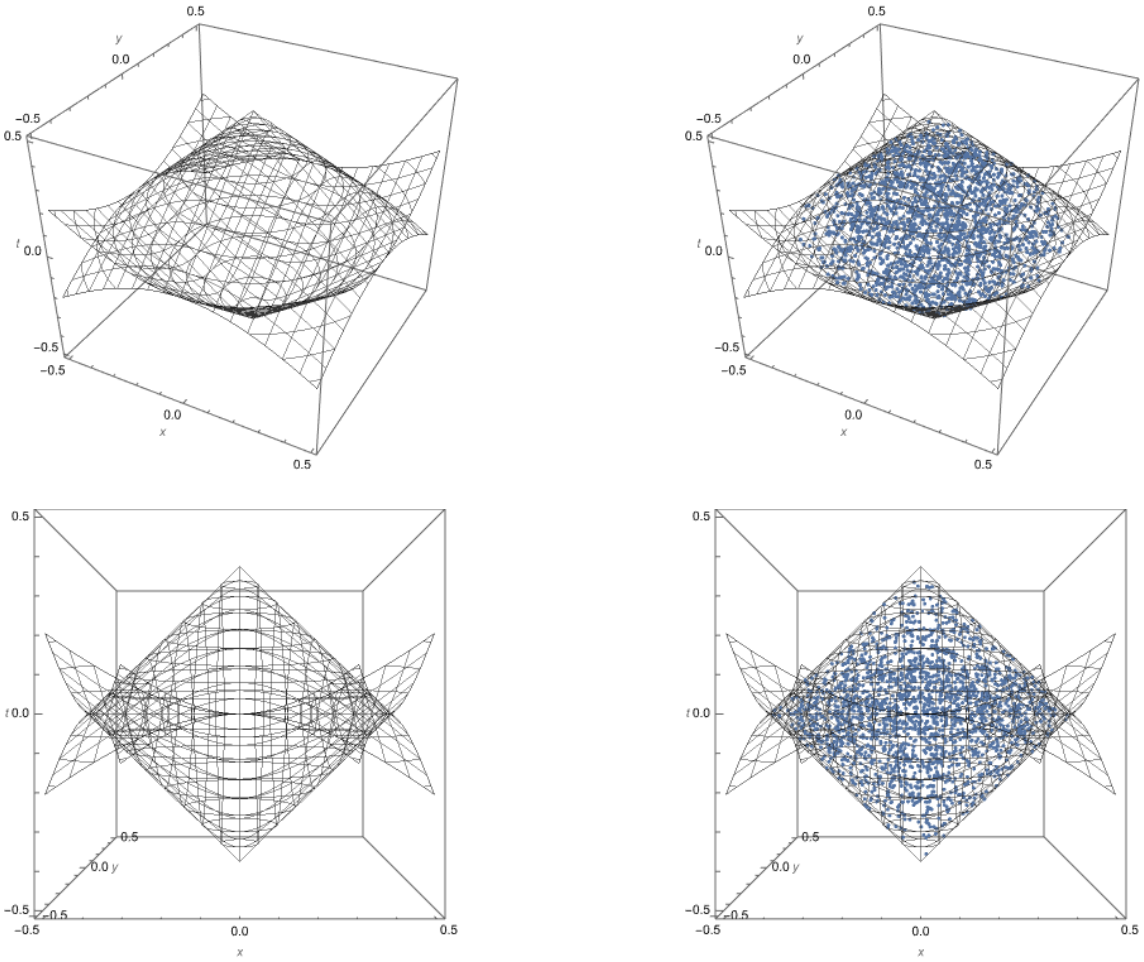

Figure 2.1: A plot of the functions $t + \sqrt{x^2+y^2} = u = h/2$ and $t - \sqrt{x^2+y^2} = v = -h/2$ along with the a causal set diamond of size $N = 2000$ and height $h = 1$.

After this change of coordinates the Pauli-Jordan function takes the simplified form;

$$\triangle(u,v) = [\theta(u) + \theta(v) - 1]\,\frac{1}{4\pi\tau}, \tag{2.24}$$

where now $\tau^2 = 2uv$, whereby

$$\triangle(u,v) = \frac{1}{4\sqrt{2}\pi}\left[\frac{\theta(u)+\theta(v)-1}{\sqrt{uv}}\right] \tag{2.25}$$

Finally, we may express (2.18) in terms of u and v as follows,

$$(i\triangle\psi)(u,v) = \int_0^{2\pi}\int_0^{\frac{h}{\sqrt{2}}}\int_0^{u} \frac{i}{8\pi}\frac{|(u-u')-(v-v')|}{\sqrt{(u-u')(v-v')}}\left[\theta(u-u')+\theta(v-v')-1\right]\psi(u',v')dv'du'd\hat{\theta}, \tag{2.26}$$

where $\hat{\theta} \equiv \theta$ has been introduced as not to cause confusion with the Dirac-delta function $\theta(x)$. We now have an equation for determining the eigenvalues and vectors using a coordinate system more suited to the space we are considering. However, equation (2.26) is difficult to solve exactly. The problem arises from the $1/\tau$ factor and the change of coordinates we have chosen doesn't help in simplifying this term. It is possible that another more complicated change of variables could help, but we will not consider any here. A potential method for finding solutions to this problem may be to consider the methods discussed in Appendix A of [37]. For such calculations it would be beneficial to know the general structure of the eigenvalues and eigenfunctions beforehand. With this in mind we now turn our attention to the discrete theory, where computational calculations of causal set operators are much easier to perform. We hope to learn about the spectrum of $i\triangle$ in a discrete setting before returning to the continuous case.

2.2.4 3D Discrete Theory

As outlined above there remains a difficulty in determining exact analytic solutions for the eigenspace spanned by $i\triangle$ in 3 dimensions; we wish to be able to solve this with the aid of causal set theory. Thus far every test of CST in the infinite density limit has agreed with the continuum. Therefore, it is reasonable to assume that clues about the behaviour of the continuous theory may be deduced from analysing the spectrum of eigenvalues and functions for the discrete counterpart of $i\triangle$. Indeed figure 5.5 in [21] demonstrates the agreement between the discrete and continuous approaches in a 2-dimensional causal diamond. It also turns out to be easier in 3-dimensions to compute causal set functions - this being a great advantage of the theory.

It remains to introduce the causal set equivalent of the theory outlined in section 2.2.2. In this thesis we follow the approach taken by Johnston in defining the causal set analogue of (2.17) via a 'stop-hop' calculation of the path integral. The main idea behind this approach is that the propagator of a particle going from one point in space-time, say from x, to another x', is determined by the complex amplitudes of a path from x to x', summed over all possible paths available to that particle [4]. This principle can be readily carried over to causal sets, where now the integrals are finite sums over all possible chains - or paths - from one causal element to another. Thinking of a particle as moving along one of these paths its amplitude of propagation may be calculated by noting how many 'stops' and 'hops' there are in that particular causal chain. Since no causal element should take precedence over any other the amplitudes for each hop should be the same at all points along the chain; similarly for amplitudes assigned to each stop. Not counting the beginning and end of points of each path, for a n-element path there are n hops with amplitude a, and $n-1$ stops with amplitude b. The total amplitude for one path of length n is therefore given by the product $a^n b^{n-1}$, from standard probability theory.
For a causal set with n elements let us define

$$\Phi := aC. \tag{2.27}$$

Then the massive propagator $K(x,x')$ from one causal element v_x to another $v_{x'}$ along a path of any length is given by

$$K := I + \Phi + b\Phi^2 + \ldots \tag{2.28}$$

$$= I + \Phi\left(I - b\Phi\right)^{-1} \tag{2.29}$$

[4] Here we are taking the particle viewpoint of quantum mechanics following Feynman's original work.

for a finite causal set. Where we note that,

$$(C^n)_{xx'} = \text{The number of chains of length } n \text{ from } v_x \text{ to } v_{x'}. \tag{2.30}$$

For the massless propagator $K_0^{(3)}$, however, one may simply take (2.17) and express it in terms of causet expressions. In [19] this was achieved by noting that the volume between two causal elements x and x' in 3-dimensions is such that $V(x-x') \propto \tau^3(x-x')$. Given that the discrete volume between two elements of the causal set v_x and $v_{x'}$ satisfies $V_{xx'} = \frac{1}{\rho}(\mathcal{C}+I)^2_{xx'}$ Johnston defines the massless propagator

$$K_0^{(3)} := \begin{cases} \frac{1}{2\pi}\left(\frac{\pi\rho}{12}\right)^{\frac{1}{3}} ((\mathcal{C}+I)^2)^{-\frac{1}{3}}_{xx'} & \text{if} \quad v_x \prec * v_y \\ 0 & \text{otherwise} \end{cases} \tag{2.31}$$

To further simplify our calculations we will utilise the association first made by Brightwell [38] and developed further by Dowker [34] whereby τ is shown to be approximated by the longest chain $l_{xx'}$ of causal elements between points x and x' such that

$$\tau = \lim_{\rho\to\infty} \langle l_{xx'} \rangle \left(\frac{\pi\rho}{12}\right)^{-1/3} \frac{1}{m_3}, \tag{2.32}$$

where,

$$m_3 = \lim_{\rho\to\infty} \langle l_{xx'} \rangle (\rho V), \qquad 1.77 \leq m_3 \leq 2.62. \tag{2.33}$$

All calculations presented in this thesis were obtained after fixing $m_3 = 1.854$. Putting all this together we are able to define the causal set Greens function,

$$K_{R\ xx'}^{(3)} := \begin{cases} \frac{m_3}{2\pi}\left(\frac{\pi\rho}{12}\right)^{1/3} \frac{1}{l_{xx'}} & \text{for} \quad x \prec x' \\ 0 & \text{otherwise} \end{cases} \tag{2.34}$$

Where $K_{R\ xx'}^{(3)}$ is a NxN matrix spanning over all N[5] elements of the the causet. Finally, we have arrived at a prescription for finding the propagator for the causet in 3 dimensions[6];

1. Sprinkle N elements onto a fixed Lorentzian manifold to create a causet via a Poisson process defined by (2.1).

2. Calculate the Causal and link matrices from (2.2) and (2.3) respectively.

3. Determine the longest chain matrix $l_{xx'}$ and the Causet propagator $K_{R\ xx'}^{(3)}$ from (2.34).

4. Determine the corresponding eigenvectors and values by diagonalising $K_{R\ xx'}^{(3)}$.

For the massive propagator one simply takes $\Phi = K_0^{(3)}$ in (2.29) and $b = \frac{m^2}{\rho}$. Having outlined the method we can now apply the prescription to a space-time of our choosing. We choose to work within the framework of a 3-dimensional.

[5] Note a change in notation, where now the size of the causet is N instead of n to avoid confusion with the notation introduced in describing the stop-hop method.

[6] This method may be easily generalised to space-times of arbitrary dimension $d > 2$ by substitution of the appropriate functions.

Causal Diamonds in 2D and Beyond

As mentioned earlier we have chosen to work within the framework of a causal set generated by a sprinkling of causal elements into $\mathbb{M}^3$. Specifically, we wish to investigate the form of the space-time propagator - by construction of a Greens function as outlined in sections 2.2.3 and 2.2.4.

3.1 2D Causal Set Theory

It will be beneficial to review the results from $\mathbb{M}^2$ as calculated by Yazdi and Sorkin as these may give us some hints about the behaviour of the propagator in higher dimensions. In [21], the propagator for 2-dimensional fixed causal diamond was studied. The benefit of choosing to study the propagator on such a structure is apparent, as every possible (causally related) path between two distinct elements in the set lies within the diamond, no information is lost outside the boundary of the diamond. An example is shown in figure 3.1 where the causal interval between two elements (being the intersection of the future and past light-cones of said elements) is completely self contained within the boundary of the diamond.

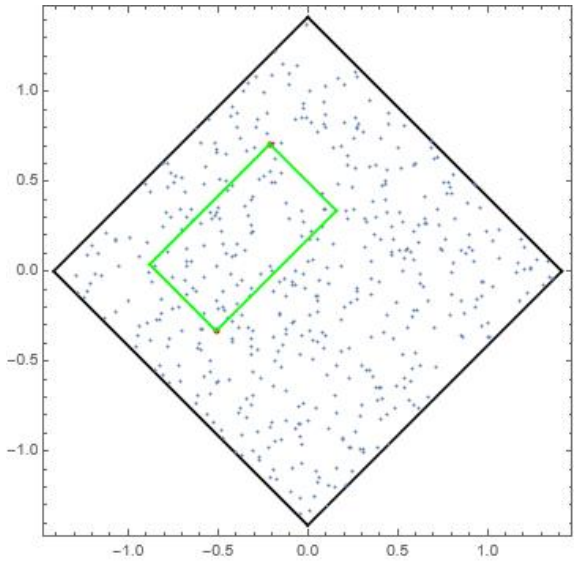

Figure 3.1: Example of causal interval - bound by solid green lines - between two elements of a sprinkled causal set of size $N = 500$, onto a 2-dimensional Minkowski background diamond - bound by solid black lines.

Staying with the 2-dimensional case it was found by Johnston that the 2-dimensional Green's function may be used to calculate the eigen-decomposition of $i\triangle$, which was shown to admit two classes of eigenfunction;

$$f_k(u,v) := e^{iku} - e^{ikv}, \quad \text{with} k = \frac{n\pi}{L}, n = \pm 1, \pm 2, \ldots \tag{3.1}$$

$$g_k(u,v) := e^{iku} + e^{ikv} - 2\cos(kL), \quad \tan(kL) = 2kL, \quad k \neq 0 \tag{3.2}$$

both with eigenvalue L/k such that,

$$(i\triangle f_k)(u,v) = \frac{L}{k} f_k(u,v), \quad (i\triangle g_k)(u,v) = \frac{L}{k} g_k(u,v). \tag{3.3}$$

where,

$$\triangle(u,v) = \frac{1}{2}(\theta(u) + \theta(v) - 1) \tag{3.4}$$

A change of variables was made such that $u = \frac{1}{\sqrt{2}}(t+x)$, and $\frac{1}{\sqrt{2}}v = (t-x)$. The corresponding causal set Pauli-Jordan function calculated by Yazdi was shown to agree with the continuum above a minimum threshold, as can be seen in figure 5.5 of [21]. For agreement with the continuous theory the causal set eigenvalues were scaled by a factor of $1/\rho$. In fact, it has been shown that $f_k(u,v)$ and $g_k(u,v)$ are the only eigenfunctions for the 2-dimensional case and span the whole space of solutions, see [19]; page 109.

3.2 3D Causal Set Theory

Now we wish to extend this scheme to the case of a 3-dimensional causal diamond, following the same reasoning as outlined in section 3.1. We start in the same way: by sprinkling elements, via a Poisson process, onto points in $\mathbb{M}^3$ restricted to the region of a causal diamond defined by the boundaries $t - \sqrt{x^2+y^2} = -\frac{h}{2}$ and $t + \sqrt{x^2+y^2} = \frac{h}{2}$, where h is the height of the diamond with volume $V = \frac{\pi h^3}{12}$. Figure 3.2 illustrates such a sprinkling of 2000 elements into a diamond of height $h = 1$.

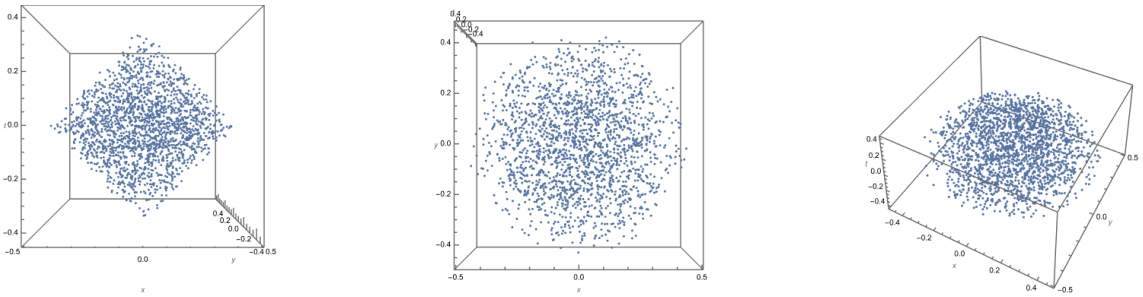

Figure 3.2: An example sprinkling of 2000 elements into a causal diamond on $\mathbb{M}^3$ of hight $h = 1$, shown from three different viewpoints.

3.2.1 Eigenvalues of Pauli-Jordan function

Following the steps outlined at the end of section 2.2.4 we are able to calculate the discrete Pauli-Jordan function and find the corresponding eigenvalues and eigenfunctions satisfying $\triangle f_n = \lambda_n f_n$, computationally. In Figure 3.3 a log-log plot of the n^{th} positive eigenvalues of the Pauli-Jordan function λ_n^+ ($\equiv \lambda$), are given against n. Just as with the positive eigenvalues of a 2-dimensional causal diamond the spectrum of eigenvalues shows a compact linear behaviour above a certain threshold, with the eigenvalues spacing out more for lower values of n. We expect to see this behaviour for much the same reasons as outlined in previous work for 2-dimensions where the non-linear behaviour is due to eigenfunction fluctuations for distances beyond the discreteness scale of the causet. Therefore, one wishes to impose a cut off to exclude these points from the spectrum. For the 2-dimensional theory this cut-off was deduced by analysing the dimensionality of λ between the continuous and discrete theories. In 3-dimensions the continuum $i\triangle$ eigenvalues $\lambda^{(3)}_{cont}$ have dimensionality of volume, whereas the causal set analogue eigenvalues $\lambda^{(3)}_{cs}$ are dimensionless. The question remains as to what space-time quantity relates the two functions?
Regarding the actual dependence of the eigenvalues on n we can simply impose a high cut-off and read the gradient of the linear part of figure 3.3 to find a power-law relation between λ_n and n. Indeed one finds $\lambda_n \propto \frac{1}{\sqrt{n}}$, whereas, for a 2-dimensional causal diamond it was found that $\lambda_n \propto \frac{1}{n}$. Once the n dependence on λ_n is known we may try and fit the spectra to a a curve of $\lambda_n = \frac{k}{\sqrt{n}}$,

for some constant k to be determined. This procedure is shown in figure 3.4 for a causal set of 200 elements sprinkled into a diamond of height $h = 1$; in this instance $k = 350.25$. One can now use this fit to approximate a more precise cut-off by looking at where the two lines in figure 3.4 diverge. We would like to make this cut-off more precise by analysing the continuum eigenvalues.

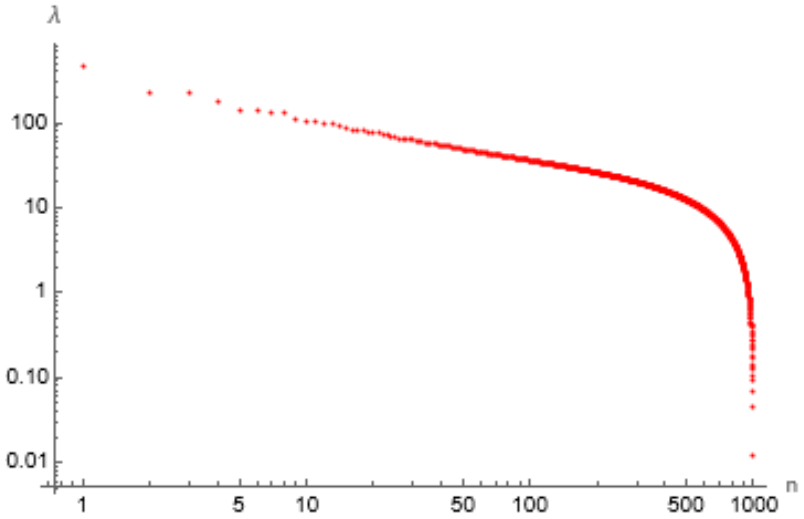

Figure 3.3: A log-log plot of the eigenvalue spectrum of the Pauli-Jordan function calculated from a causet of 2000 elements - sprinkled into a causal diamond of height $h = 1$ in $\mathbb{M}^3$.

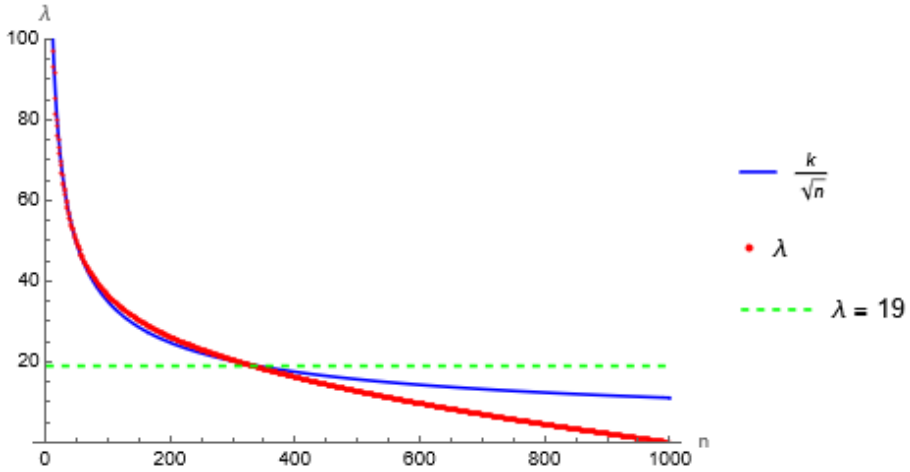

Figure 3.4: The eigenvalues λ are plotted against n for a 2000 element causal set of height $h = 1$ and compared to the function $k/\sqrt{n}$ with $k = 350.25$. Agreement is shown up to a value of $\lambda = 19$ represented by the dashed line.

So far we have only presented data of a 2000 element causal diamond of height $h = 1$. However, we would also like to know whether the spectra of $i\triangle$ depends on the density of the causet, or indeed the size of the causal diamond itself. We would expect some dependence on the density ρ up to a point where the theory should level off to agree with the continuous case - this being the high density limit. However, the sensitivity of this progression is something which one may investigate further for clues to the precise analytic dependence of the spectra in the continuous case. Figure 3.5 is a log-log plot of the eigenvalues of $i\triangle$ for causal sets of $h = 1$, with density $\rho = \{\frac{12000}{\pi}, \frac{24000}{\pi}, \frac{36000}{\pi}, \frac{48000}{\pi}, \frac{60000}{\pi}, \frac{72000}{\pi}, \frac{84000}{\pi}, \frac{96000}{\pi}\}$, from left to right respectively. As one might expect the eigenvalues for of the Pauli-Jordan function tend to differ less and less as the density increases and the spectra tend toward the continuous limit. Since this bunching can be seen for a causal diamond of 8000 elements it is reasonable to assume for a diamond of height

$h = 1$ a sprinkling of 10,000-20,000 elements should yield results which can be compared to the continuous case - after an truncation has been performed to remove the smallest eigenvalues of $i\triangle$.

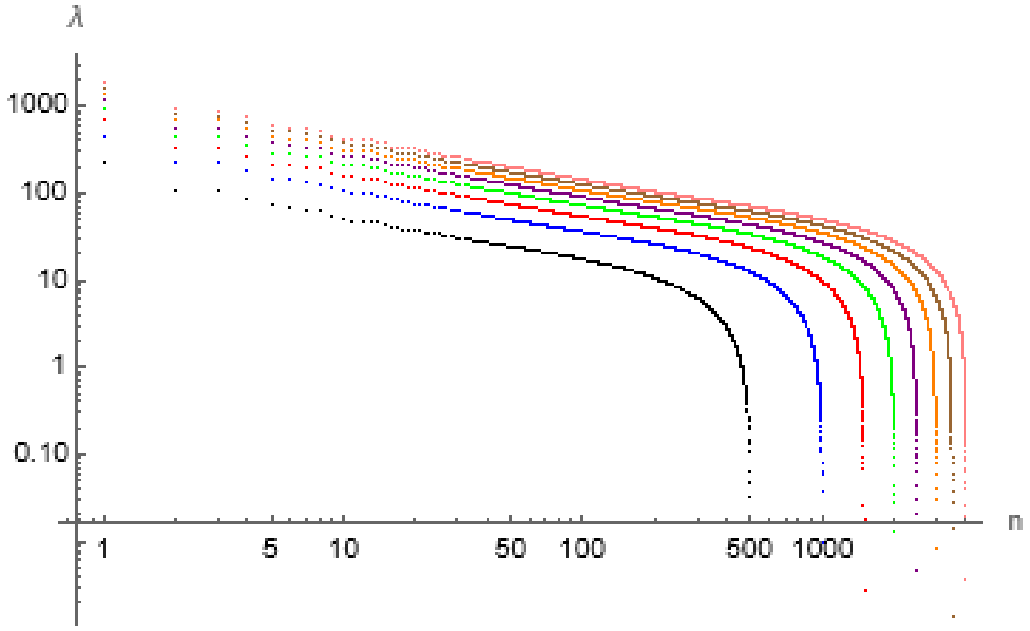

Figure 3.5: eigenvalues of $i\triangle$ for causal sets of $h = 1$, with density ρ increasing from $\rho = 12,000/\pi$ to $\rho = 96,000/\pi$ in steps of $12,000/\pi$ from left to right.

In as far as one can analyse the spectrum of eigenvalues of $i\triangle$ we have two immediate questions we would like to answer:

How many independent functions make up the full spectrum of eigenvalues?

For the 2-dimensional case it can be seen from (3.1) and (3.2) that there are two independent functions of eigenvalues which have been shown to make up the full spectrum. Naturally one would like to know how many independent functions make up the full spectrum in 3-dimensions? One potential way to discern exactly how many functions there are is to analyse the periodicity or composite periodicity of the spectrum.

What is the factor in relating between continuum and causal set eigenvalues?

As mentioned in the previous chapter the continuum Greens function has dimensions of volume - as it is a measure relating to the causal interval between two space-time points. For the discrete theory, however, the propagator is dimensionless so a purely space-time factor[1] of relevant dimension is needed if calculations between the two theories are to agree in the high density limit. One such candidate is the density ρ. It is known that for the case of 2-dimensions $\lambda_{con} = \lambda_{cs}/\rho$. This begs the question of what this factor may be for three dimensions; could it be a power of ρ or a combination of ρ with some other expressions?

[1] By this we mean intrinsic properties of the space-time for which causal set analogues are well defined.

3.2.2 Eigenfunctions of the Pauli-Jordan function

As well as studying the form of the eigenvalues, as was done in the previous section, one may also investigate the eigenfunctions of $i\triangle$ obtained by direct computation of the causal set. The analytic eigenfunctions of 2-dimensions are given by (3.1) and (3.2). Let us first start by applying the steps outlined in section 2.2.4 to a 2-dimensional causal diamond to find the causal set eigenfunctions as was done in [21].

In figure 3.6 the real parts of $f_k(u,v)$ and $g_k(u,v)$ are shown plotted together for the values of $k = 1, 2, 3, 4$ respectively, for a 2-dimensional causal diamond where we have taken $L = 1$. Let us then compare this with the eigenfunctions of the Pauli-Jordan function as calculated from a causal set of 1000 elements and density $\rho = 250$. After diagonalizing the propagator one is left with 1000 eigenvalues and eigenvectors. Choosing to focus on pairs of adjacent eigenvectors we can see an immediate correlation between the discrete and continuous functions. For a causal set of size N we take the set of all N eigenvectors to be V such that $V = v_1, v_2, \ldots v_N$, then each $v_i \in V$ is a list of 2-dimensional coordinates of length N. Denoting then the i^{th} and j^{th} pair of eigenvectors in V to be (v_i, v_j), we have in figure 3.7 the real parts of the superimposed plots for $(a) : (v_2, v_3)$, $(b) : (v_6, v_7)$. $(c) : (v_9, v_{10})$ and $(d) : (v_{11}, v_{12})$.

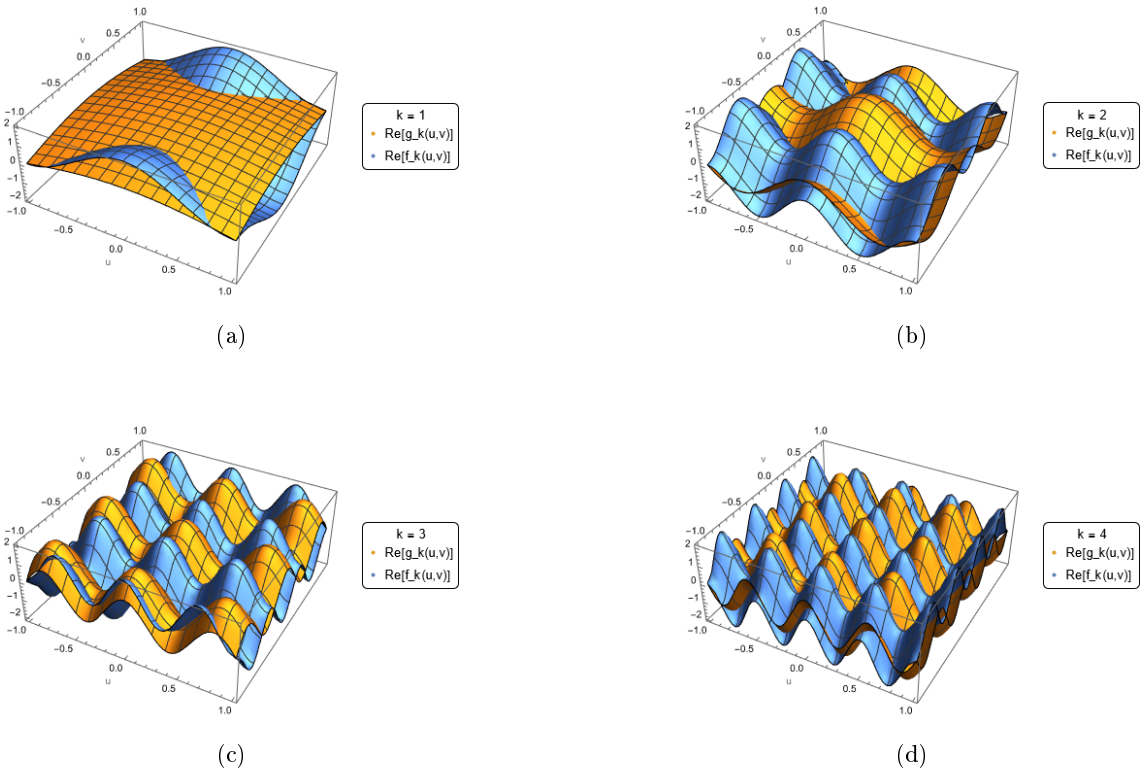

(a) (b)

(c) (d)

Figure 3.6: The real parts of $f_k(u,v)$ and $g_k(u,v)$ plotted together for values of $(a) : k{+}1$, $(b) : k{+}2$, $(c) : k+3$ and $(d) : k+4$ for a diamond of Length $L = 1$.

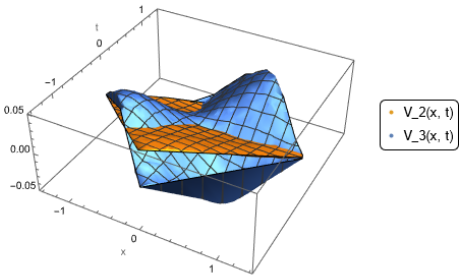

(a) (v_2, v_3)

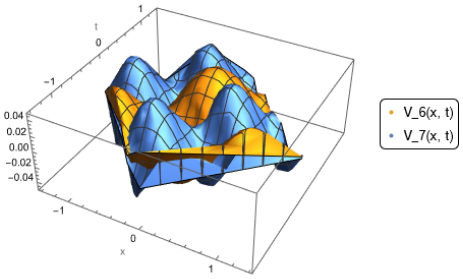

(b) (v_6, v_7)

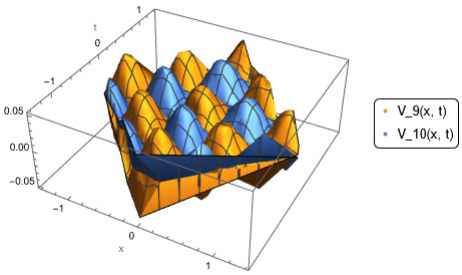

(c) (v_9, v_{10})

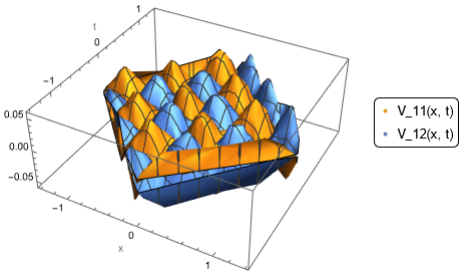

(d) (v_{11}, v_{12})

Figure 3.7: The real parts of eigenvectors $(a) : (v_2, v_3)$, $(b) : (v_6, v_7)$. $(c) : (v_9, v_{10})$ and $(d) : (v_{11}, v_{12})$ plotted for a causal diamond of length $L = 1$ and size $N = 1000$

So far we have only visualised the results already obtained by Yazdi and have done nothing new. However, what the above does is illustrate again how results from a causal framework may be used to investigate the continuous counterpart and visa versa. When going up to 3-dimensions we know that the problem of solving the eigenfunctions and values of the Pauli-Jordan function becomes much harder, primarily due to the addition of $1/\tau$ in the retarded Greens function. However, it could also be possible that the behaviour of the eigenfunctions show similarities with those of two dimensions when one looks at cross-sections in the spatial planes. If so then an appropriate ansatz may be used to simplify the problem. It is also interesting to ask if there is any symmetry in the functions as this may ease the difficulty of finding exact solutions to 3-dimensional continuous theories.

In order to analyse the 2-dimensional behaviour of the 3-dimensional eigenfunction we need to define an appropriate cross-section of the causal diamond. As the set is not continuous we cannot simply take an exact cross-section as this would have a very low probability of containing any causal elements. Instead, we require a slice of thickness b to retrieve a 'block diamond' of a 2-dimensional surface. Such an example of this is illustrated in figure 3.8. To determine the behaviour of the functions under investigation slices of both the spatial directions x and y are taken - first centred in the middle of the diamond such that the midpoint of the slice is aligned with the origin of the respective axes. This is done to begin with as, the closer to the origin the more causal set elements there will be contained within the slice. Slices centred about planes further from the origin will be of smaller causal diamonds; the size of these diamonds may then effect the behaviour of the spectrum of $i\triangle$. For an accurate comparison one would need to study slices analogous to the size of a 2-dimensional diamond with a similar density of points. As mentioned earlier a causal diamond of 10,000 - 20,000 elements should give reliable results to analyse for a diamond of height $h = 1$.

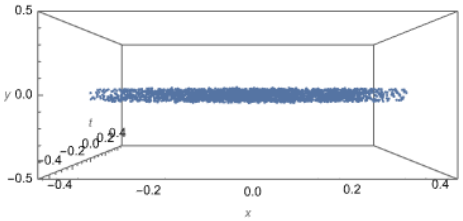

(a) $\{0, -2, 0\}$

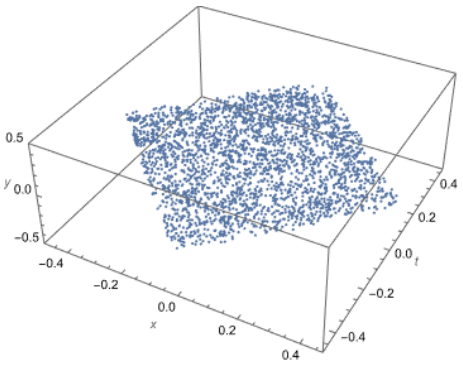

(b) $\{1.3, -2.4, 2\}$

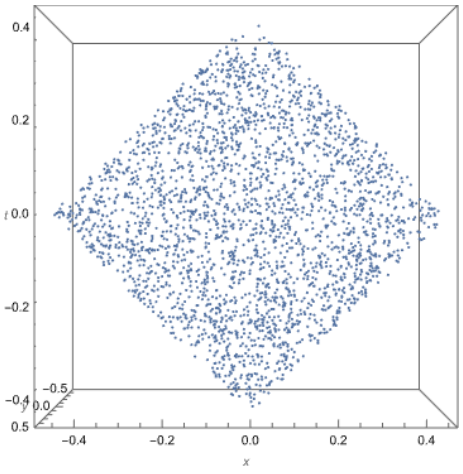

(c) $\{0, 0, 2\}$

Figure 3.8: An example of a cross-section taken from a 15,000 element causal set with the slice taken in the x, t plane centred about $y = 0$, where $b = 0.1$ and $N_R = 2807$.

We choose to take cross-sections of a 15,000 element causal set of density $\rho = 180'/\pi$. We also require quite a large density causet, as this reduces the interference that is inevitable when performing a cross-section of this nature. An example of how the cross-sections change due to the location of the plane slice are shown in figure 3.9. To properly analyse the dependence of the functions on the position of the cross-section, one would need to look at increasingly large sets as to keep the number of elements at each section within the same order of magnitude. Due to the symmetry of the causal diamond between the x and y directions we see that cross-sections taken in the (y, t) exhibit the same dependence on position.

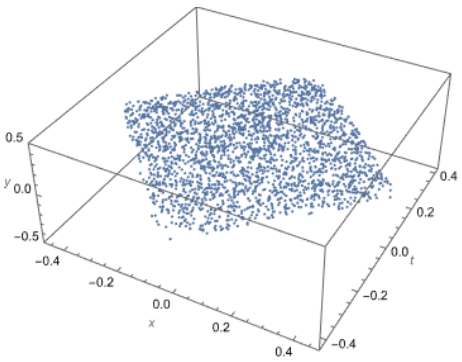

(a) (x,t) plane at $y = 0.1$, $N_R = 2533$

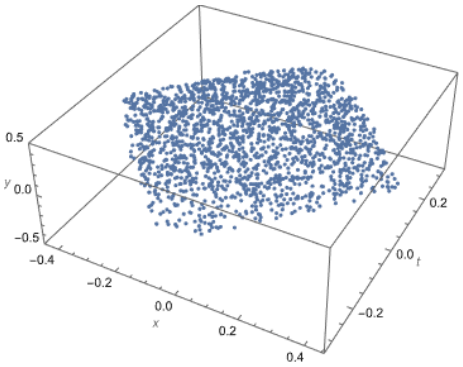

(b) (x,t) plane at $y = 0.2$, $N_R = 1908$

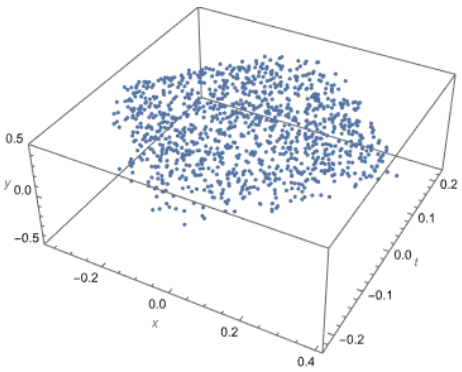

(c) (x,t) plane at $y = 0.3$, $N_R = 1134$

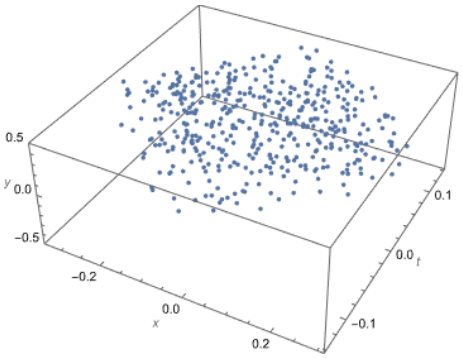

(d) (x,t) plane at $y = 0.4$, $N_R = 446$

Figure 3.9: Slice of thickness $b = 0.1$, taken on the (x,t) plane at $y = \{0.1, 0.2, 0.3, 0.4\}$ of a causal set of size $N = 15,000$. Where N_R is the size of the reduced causal set contained within the boundaries of the cross-section.

Keeping in mind the form of the eigenfunctions for $i\triangle$ as seen in figures 3.6 and 3.7, for 2-dimensions, we now look at the eigenfunctions in 3-dimensions for cross-sections of thickness $b = 0.1$ on a $N = 15,000$ causal set, such that $N_R = 2807$.[2] In order to show the form of the functions clearly, plots are given of only one eigenvector at a time. Figure 3.10 shows the 3-dimensional representation of a the eigenvectors v_7, v_{15}, v_{27}, v_{35}, v_{45} and v_{57} defined in the same way as previously.[3] A 2-dimensional density plot of the corresponding functions is presented in figure 3.11.

Looking at figures 3.10 and 3.11 it is clear the the eigenfunctions for these cross-sections show similar traits to those in figures 3.6 and 3.7; both demonstrate periodic behaviour with increasing frequency. This is encouraging to see as it suggest that the form of the eigenfunctions may be similar to those of the 2D theory when taken in isolation. Due to the symmetry of the problem it is also noted that the eigenfunctions for the other spatial direction shares similar characteristics when analysed. This leads to the possibility that the eigenfunctions of the 3-dimensional Pauli-Jordan operator are comprised of the superposition of eigenfunctions of the corresponding 2-dimensional theory. There could also exist other terms dependent on the whole 3-dimensional space and not seen in lower dimensions.

As eluded to in 2.2.3 a method for determining the eigenvalues of $i\triangle$ as discussed in Appendix A of [37] utilises a complete basis of states to iteratively find eigenvalues and eigenfunctions. This method may not always simplify the problem or produce analytically 'tidy' functions as seen in (3.1) and (3.2). However, if one has an insight into the form that the eigenfunctions may take, then choosing an appropriate complete basis should make the process more efficient. It has been shown that the spectrum of $i\triangle$ in 3-dimensions shares similarities to the 2D case (for appropriately defined cross-sections), such that the eigenfunctions resemble plane waves in $\mathbb{M}^2$. Then it could also be beneficial to try a 3D plane-wave basis of states. The 3D plane-wave basis forms a complete basis, as well as the added bonus of being easily reduced to lower dimensions by ignoring behaviour in one or more of the spatial directions.

Analysing the eigenfunctions found for the discrete theory could also allow one to determine how many independent periodic functions make up the whole spectrum of $i\triangle$. As with the 2D case the eigenvectors dependence on n may be related to the to the wave-number k, of the functions. The exact relation of n to k is something which would be of interest for further study. One could use the results above to help determine the periodicity of n, as well as the methods outlined in section 3.2.1 - which suggest using eigenvalues to find the periodicity of n and its relation to the wave-number.

[2] N_R is the size of the reduced causet obtained from taking slices of the original causet of size N.

[3] The plots are presented as 3-dimensional scatter plots as the noise due to the nature of the cross-section limits the interpolating capabilities of Mathematica 12.3.1.

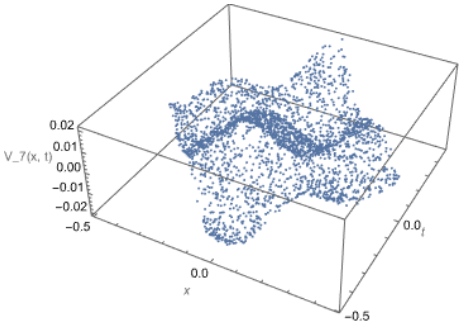

(a) v_7

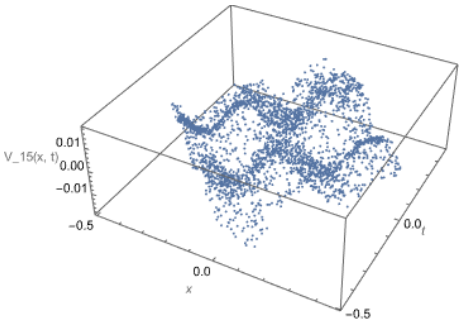

(b) v_{15}

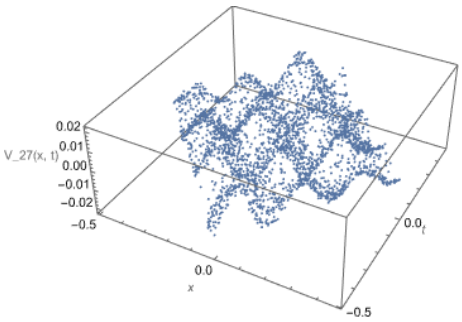

(c) v_{27}

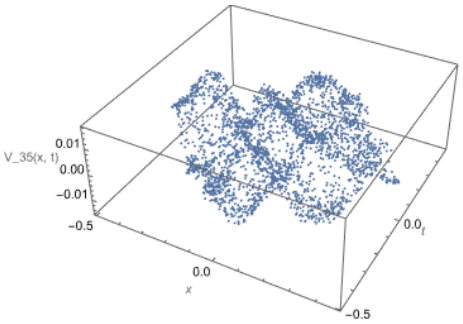

(d) v_{35}

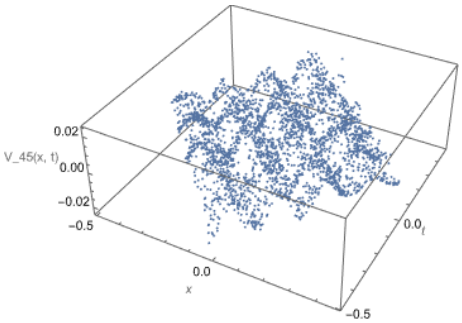

(e) v_{45}

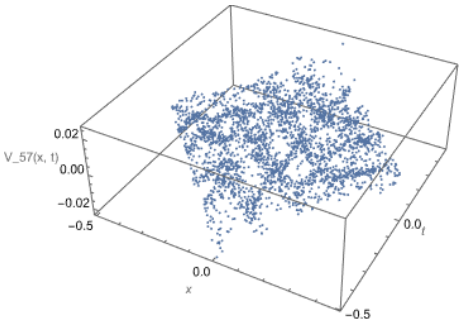

(f) v_{57}

Figure 3.10: A 3D scatter plot of the eigenfunctions $(a) = v_7$, $(b) = v_{15}$,$(c) = v_{27}$, $(d) = v_{35}$, $(e) = v_{45}$ and $(f) = v_{57}$ for a reduced causal diamond of size $N_R = 2807$ obtained after taking a cross-sectional slice of a $N = 15,000$ causet in the (x, t) plane centred at $y = 0$.

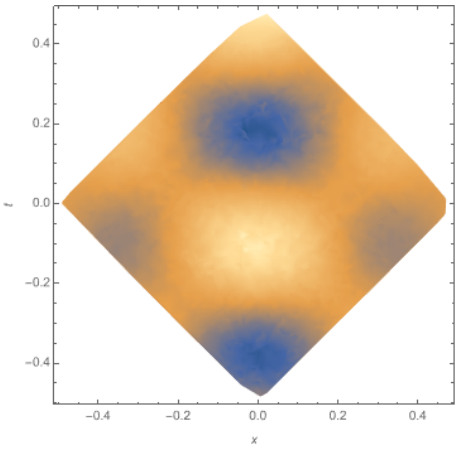

(a) v_7

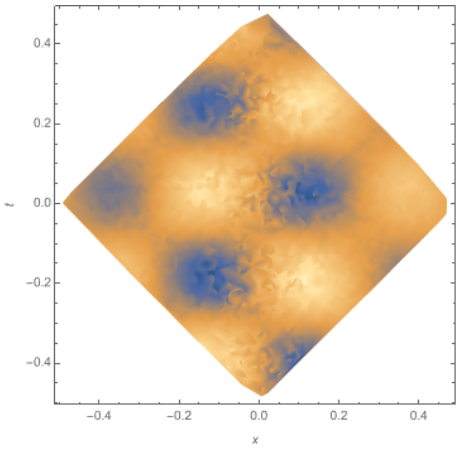

(b) v_{15}

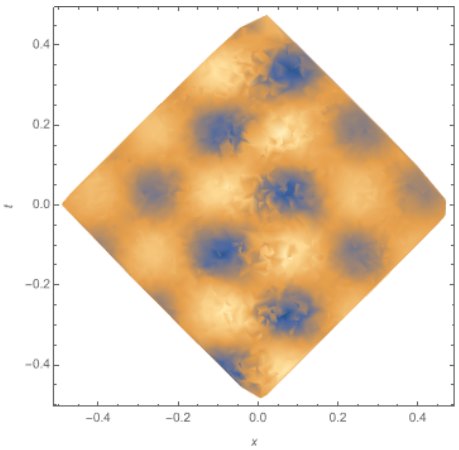

(c) v_{27}

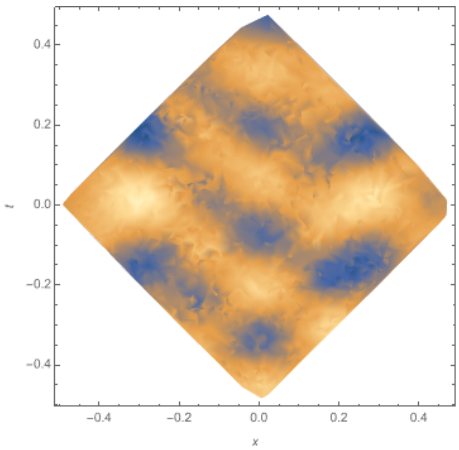

(d) v_{35}

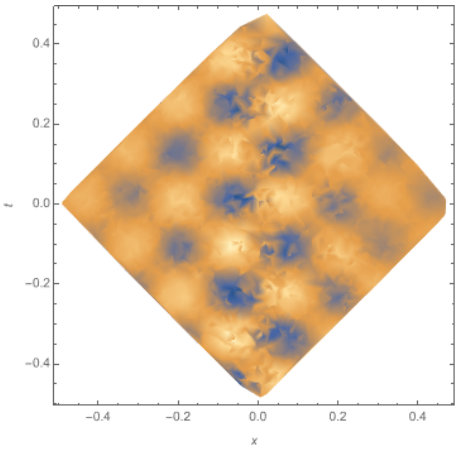

(e) v_{45}

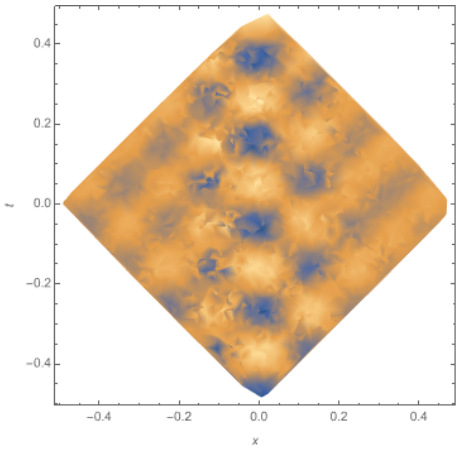

(f) v_{57}

Figure 3.11: A 2D density plot of the eigenfunctions $(a) = v_7$, $(b) = v_{15}$,$(c) = v_{27}$, $(d) = v_{35}$, $(e) = v_{45}$ and $(f) = v_{57}$ for a reduced causal diamond of size $N_R = 2807$, obtained after taking a cross-sectional slice of a $N = 15,000$ causet in the (x, t) plane centred at $y = 0$.

Conclusion

In the quest to find a theory of Quantum Gravity, physicists have been led to question the very nature of space and time in which the universe unfolds. The ideas of Einstein's Special and General Relativity changed the way in which scientists imagined these concepts and their relationship to each other. Since then, great success has been made in evolving these principles into rigorous mathematical frameworks of Geometry and Topology. The introduction of the so called 'Standard Model' of particle physics and the development of Quantum Field Theory again furthered our understanding of how matter behaved and interacted in nature. Now at the beginning of the 21st century physicists and mathematicians are again questioning our understanding of space and time. Causal set theory has emerged as a seemingly natural way to explain many of the problems facing modern physics. Although still in its infancy, great success has been made in relating ideas of discrete and continuous theories.

In this thesis the foundations and motivations of causal set theory have been outlined and a basic review of the theory has been presented. Ideas about how one might represent a causet via a sprinkling of space-time elements have been presented, as well as calculating such a causet for a 3-dimensional causal diamond in 2+1 Minkowski space. A review of the work done in defining a quantum field theory via the so called Sorkin-Johnston approach has been discussed. The potential for using causets to make breakthroughs in continuum theories has been eluded to throughout the work. With this in mind the eigenvalues and eigenfunctions of the Pauli-Jordan operator for this space were calculated via computation methods outlined in section 2.2.4. These quantities are as yet undefined in the continuous theory, and it is hoped that causal sets may provide useful insights to this unknown. Indeed, the eigenfunctions show a close resemblance to the 2-dimensional theory - for which precise analytic functions have been found - when appropriate cross-sections were taken.

Using the known form of the eigenvalues and eigenvectors of $i\triangle$ from analysis of causal set operators defined in section 2.2.4, further questions arise about how the continuous spectrum may appear. Future avenues of research could be conducted in this area. Specifically, one may ask what dimensional parameters need to be included to scale the eigenvalues if agreement is to be made between the two approaches. As well as this, one may investigate how many independent functions make up the full spectrum by looking at the periodicity of both the eigenvalues and eigenfunctions found. With continuing research one could look to investigate the relationship between n and k.

Having elevated the theory to 3-dimensions we now have a better understanding of the form that $i\triangle$ may take. Further research in this area is sure to expand our understanding of both continuous and discrete theories, and ultimately allow us to gain greater knowledge of the importance of causality at the most fundamental level.

Bibliography

[1] Rafael D. Sorkin. Forks in the road, on the way to quantum gravity. *Int. J. Theor. Phys.*, 36 (12):2759–2781, 1997. ISSN 00207748. doi: 10.1007/BF02435709.

[2] Pietro Doná and Simone Speziale. Introductory lectures to loop quantum gravity. jul 2010. URL `http://arxiv.org/abs/1007.0402`.

[3] Joseph Gerard Polchinski. String theory. Joseph Polchinski. *Cambridge Monogr. Math. Phys.*, 2005.

[4] Eitan Bachmat. Discrete spacetime and its applications. pages 347–359. 2008. doi: 10.1090/conm/458/08946.

[5] Luca Bombelli, Joohan Lee, David Meyer, and Rafael D Sorkin '. Space-Time as a Causal Set. 59(5), 1987.

[6] Fay Dowker. Causal sets and the deep structure of spacetime. In *100 Years Relativ. Space-Time Struct. Einstein Beyond*, pages 445–464. World Scientific Publishing Co., jan 2005. ISBN 9789812700988. doi: 10.1142/9789812700988_0016.

[7] E. H. Kronheimer and R. Penrose. On the structure of causal spaces. *Math. Proc. Cambridge Philos. Soc.*, 63(2):481–501, 1967. ISSN 14698064. doi: 10.1017/S030500410004144X.

[8] Cristopher Moore. Comment on Space-time as a causal set, 1988. ISSN 00319007.

[9] Rafael D. Sorkin. Causal Sets: Discrete Gravity (Notes for the Valdivia Summer School). sep 2003. URL `https://arxiv.org/abs/gr-qc/0309009v1`.

[10] S. W. Hawking and G. F. R. Ellis. The Large Scale Structure of Space-Time. *Large Scale Struct. Space-Time*, may 1973. doi: 10.1017/CBO9780511524646. URL `https://www.cambridge.org/core/books/large-scale-structure-of-spacetime/1E6B961EC9878EDDBBD6AC0AF031CC93`.

[11] Jacob D. Bekenstein. Black holes and entropy. *Phys. Rev. D*, 7(8):2333–2346, 1973. ISSN 05562821. doi: 10.1103/PhysRevD.7.2333.

[12] S. W. Hawking. Black holes and thermodynamics. *Phys. Rev. D*, 13(2):191–197, 1976. ISSN 05562821. doi: 10.1103/PhysRevD.13.191.

[13] Luca Bombelli, Rabinder K. Koul, Joohan Lee, and Rafael D. Sorkin. Quantum source of entropy for black holes. *Phys. Rev. D*, 34(2):373–383, 1986. ISSN 05562821. doi: 10.1103/PhysRevD.34.373.

[14] D. Dou. Causal Sets, a Possible Interpretation for the Black Hole Entropy,and Related Topics. jun 2001. URL `http://arxiv.org/abs/gr-qc/0106024`.

[15] Mehdi Saravani, Rafael D. Sorkin, and Yasaman K. Yazdi. Spacetime entanglement entropy in 1 + 1 dimensions. *Class. Quantum Gravity*, 31(21), nov 2014. ISSN 13616382. doi: 10.1088/0264-9381/31/21/214006.

[16] G. 't Hooft. Quantum Gravity: A Fundamental Problem and Some Radical Ideas. *Recent Dev. Gravit.*, pages 323–345, 1979. doi: 10.1007/978-1-4613-2955-8_8. URL `https://link.springer.com/chapter/10.1007/978-1-4613-2955-8{_}8`.

[17] R Sorkin. Spacetime and causal sets. *J.C. D'Olivo, E. Nahmad-Achar, M. Rosenbaum, M.P. Ryan, L.F. Urrutia, F. Zertuche (Eds.), Relativ. Gravit. Class. Quantum, Proc. SILARG VII Conf. Cocoyoc, Mex. December 1990, World Sci. Singapore, 1991*, pages 150–173. URL http://www.perimeterinstitute.ca/personal/rsorkin/some.papers/66.cocoyoc.pdf.

[18] Fay Dowker and Stav Zalel. Evolution of Universes in Causal Set Cosmology. mar 2017. doi: 10.1016/j.crhy.2017.03.002. URL http://arxiv.org/abs/1703.07556http://dx.doi.org/10.1016/j.crhy.2017.03.002.

[19] Steven Johnston. Quantum Fields on Causal Sets. oct 2010. URL http://arxiv.org/abs/1010.5514.

[20] Rafael D. Sorkin. From Green Function to Quantum Field. *Int. J. Geom. Methods Mod. Phys.*, 14(8), mar 2017. doi: 10.1142/s0219887817400072. URL https://arxiv.org/abs/1703.00610v1.

[21] Rafael D. Sorkin and Yasaman Kouchekzadeh Yazdi. Entanglement entropy in causal set theory. *Class. Quantum Gravity*, 35(7), 2018. ISSN 13616382. doi: 10.1088/1361-6382/aab06f.

[22] Dionigi M. T. Benincasa and Fay Dowker. The Scalar Curvature of a Causal Set. *Phys. Rev. Lett.*, 104(18), jan 2010. doi: 10.1103/physrevlett.104.181301. URL https://arxiv.org/abs/1001.2725v4.

[23] David B. Malament. The class of continuous timelike curves determines the topology of spacetime. *J. Math. Phys.*, 18(7):1399–1404, 1976. ISSN 00222488. doi: 10.1063/1.523436.

[24] S. W. Hawking, A. R. King, and P. J. McCarthy. A new topology for curved space-time which incorporates the causal, differential, and conformal structures. *J. Math. Phys.*, 17(2):174–181, 1975. ISSN 00222488. doi: 10.1063/1.522874.

[25] Seth Major, David Rideout, and Sumati Surya. On recovering continuum topology from a causal set. *J. Math. Phys.*, 48(3), 2007. ISSN 00222488. doi: 10.1063/1.2435599.

[26] D. P. Rideout and R. D. Sorkin. Classical sequential growth dynamics for causal sets. *Phys. Rev. D - Part. Fields, Gravit. Cosmol.*, 61(2), 2000. ISSN 15502368. doi: 10.1103/PhysRevD.61.024002.

[27] D. P. Rideout. Evidence for a continuum limit in causal set dynamics. *Phys. Rev. D*, 63(10), 2001. ISSN 05562821. doi: 10.1103/PhysRevD.63.104011.

[28] Jonathan Gorard. Algorithmic Causal Sets and the Wolfram Model. nov 2020. URL http://arxiv.org/abs/2011.12174.

[29] Fay Dowker, Joe Henson, and Rafael D. Sorkin. Quantum gravity phenomenology, Lorentz invariance and discreteness. *Mod. Phys. Lett. A*, 19(24):1829–1840, aug 2004. ISSN 02177323. doi: 10.1142/S0217732304015026.

[30] P A M Dirac. The Principles of Quantum Mechanics (1995 reprint of 4th ed). 1930. URL http://www.worldcat.org/isbn/0198520115.

[31] Steven Weinberg. The Quantum Theory of Fields. *The Quantum Theory of Fields*, jun 1995. doi: 10.1017/CBO9781139644167. URL https://www.cambridge.org/core/books/quantum-theory-of-fields/22986119910BF6A2EFE42684801A3BDF.

[32] R. P. Feynman. Space-time approach to non-relativistic quantum mechanics. *Rev. Mod. Phys.*, 20(2):367–387, 1948. ISSN 00346861. doi: 10.1103/RevModPhys.20.367.

[33] Rafael D. Sorkin. Scalar Field Theory on a Causal Set in Histories form. In *J. Phys. Conf. Ser.*, volume 306. Institute of Physics Publishing, 2011. doi: 10.1088/1742-6596/306/1/012017.

[34] S. Nomaan Ahmed, Fay Dowker, and Sumati Surya. Scalar field Green functions on causal sets. *Class. Quantum Gravity*, 34(12), may 2017. ISSN 13616382. doi: 10.1088/1361-6382/aa6bc7.

[35] R. E. PEIERLS. The commutation laws of relativistic field theory. pages 367–382. apr 1997. doi: 10.1142/9789812795779_0039. URL http://www.worldscientific.com/doi/abs/10.1142/9789812795779{_}0039.

[36] Steven Johnston. Feynman Propagator for a Free Scalar Field on a Causal Set. *Phys. Rev. Lett.*, 103(18), oct 2009. ISSN 00319007. doi: 10.1103/PhysRevLett.103.180401.

[37] Fay Dowker. Boundary contributions in the causal set action. *Class. Quantum Gravity*, 38 (7), apr 2021. ISSN 13616382. doi: 10.1088/1361-6382/abc2fd.

[38] Graham Brightwell and Ruth Gregory. Structure of random discrete spacetime. *Phys. Rev. Lett.*, 66(3):260–263, jan 1991. ISSN 0031-9007. doi: 10.1103/PhysRevLett.66.260. URL `https://link.aps.org/doi/10.1103/PhysRevLett.66.260`.